TOPOLOGICAL ASYMPTOTIC ANALYSIS OF KIRCHHOFF'S PLATE BENDING PROBLEM APPLIED IN THE CONTEXT OF STRUCTURAL TOPOLOGY DESIGN

A. A. Novotny, novotny@lncc.br
S. M. Giusti, giusti@lncc.br
D. E. Campeão, dcampeao@lncc.br
Laboratório Nacional de Computação Científica - LNCC/MCT, Av. Getúlio Vargas 333, 25651-075 Petrópolis - RJ, Brasil

Abstract. *The aim of this work is to present the calculation of the topological derivative for the total potential energy associated to the Kirchhoff's plate bending problem, when a circular inclusion is introduced at an arbitrary point of the domain. By using classical shape sensitivity together with asymptotic analysis of the solution, we obtain a closed formula for the topological sensitivity. For the sake of completeness, the analytical expression for the topological derivative is checked numerically using the standard finite element method. Then, we use the obtained sensitivity as a descent direction in a topology design algorithm which allows to simultaneously remove and insert material. Finally, we explore this feature showing a numerical experiment concerning structural topology design within the context of Kirchhoff's plate bending problem.*

Keywords: *Topological derivative, Kirchhoff's plate, topology optimization.*

1. INTRODUCTION

The topological asymptotic analysis provides the sensitivity of a given shape functional with respect to an infinitesimal singular domain perturbation, like the insertion of holes, inclusions, source-term or cracks. Therefore, this sensitivity can be naturally used as a descent direction in an optimization algorithm. The topological derivative can be seen as an extension of the classical notion of derivative. It has been rigorously introduced by Sokołowski and Żochowski (1999). Since then, the topological derivative concept has proved extremely useful in the treatment of a wide range of problems topology optimization (Allaire et al. (2005),Amstutz and Andrä (2006),Lee and Kwak (2008)), inverse analysis (Feijóo (2004),Amstutz et al. (2005)) and image processing (Auroux et al. (2007), Larrabide et al. (2008)) and has become a subject of intensive research. Concerning the theoretical development of the topological asymptotic analysis, the reader may refer to Nazarov and Sokołowski (2003), for instance.

In order to introduce these concepts, let us consider an open bounded domain $\Omega \subset \mathbb{R}^2$, which is submitted to a non-smooth perturbation in a small region $\omega_\epsilon(\hat{x}) = \epsilon\omega(\hat{x})$ of size ϵ with center at an arbitrary point $\hat{x} \in \Omega$. Thus, we assume that a given shape functional ψ admits the following topological asymptotic expansion

$$\psi(\Omega_\epsilon) = \psi(\Omega) + f(\epsilon)D_T(\hat{x}) + o(f(\epsilon)) \ , \tag{1}$$

where Ω_ϵ is the topologically perturbed domain and $f(\epsilon)$ is a positive function that decreases monotonically such that $f(\epsilon) \to 0$ when $\epsilon \to 0$. Then, the term $D_T(\hat{x})$ is defined as the topological derivative of ψ. Therefore, this derivative can be seen as a first order correction on $\psi(\Omega)$ to estimate $\psi(\Omega_\epsilon)$. In addition, from Eq. (1), we have that the classical definition of the topological derivative is given by

$$D_T\left(\hat{x}\right) = \lim_{\epsilon \to 0} \frac{\psi\left(\Omega_\epsilon\right) - \psi\left(\Omega\right)}{f\left(\epsilon\right)} \ . \tag{2}$$

In Novotny et al. (2005) is presented the calculation of the topological derivative for the total potential energy associated to the Kirchhoff's plate bending problem, when the domain is perturbed by the introduction of an infinitesimal hole with homogeneous Neumann boundary condition. Then, in this work we extend the above result considering as topological perturbation the nucleation of an infinitesimal circular inclusion with another material property.

This paper is organized as follows. Section 2 describes the model associated to the Kirchhoff's plate bending problem. The topological sensitivity analysis of the total potential energy associated to the problem under consideration is developed in Section 3, where the main result of the paper is presented: a closed formula for the topological derivative. In addition, a simple finite element-based numerical example is also provided for the numerical verification of the analytically derived topological derivative formula. In section 4 is presented a numerical experiment showing the potentiality of the presented methodology in the context of topological optimization. The paper ends in Section 5 where concluding remarks are presented.

2. FORMULATION OF THE PROBLEM

Let us review briefly in this section the theory of elastic plates under Kirchhoff's assumptions. Thus, we consider a flat plate, with thickness $\rho \in \mathbb{R}^+$ (admitted constant for the sake of simplicity), characterized by the two-dimensional domain $\Omega \subset \mathbb{R}^2$, which is submitted to bending effects. In order to model this phenomenon Kirchhoff developed, in 1850, a theory based on the following *ad-hoc* kinematic assumptions:

> *The normal fibers to the middle plane of the plate remain normal during deformation and do not suffer variations in their length.*

Consequently, both transversal shear and normal deformations are null. This fact limits the application of Kirchhoff's approach on plates whose deflections are small in relation to the thickness ρ. Note that in the presence of concentrated loads or defects like cracks, additional care shall be necessary since transversal shear deformation may be significative.

Using the kinematic assumptions introduced by Kirchhoff and adopting the constitutive relation for a linear elastic isotropic material, we have the following resultant moment and plate curvature relation

$$M = -\mathbb{C}\nabla\nabla u \ , \tag{3}$$

where the scalar field u denotes the transverse displacement (deflection), the second order tensor $\nabla\nabla u$ represents the change of curvature of the plate, the symmetric tensor M represents the resultant bending moment acting in the middle plane of the plate and $\mathbb{C}$ represents the fourth order elasticity tensor integrated through the plate thickness, given by

$$\mathbb{C}=\frac{E\rho^3}{12\left(1-\nu^2\right)}\left[\left(1-\nu\right)\mathbb{I}+\nu\left(I\otimes I\right)\right] \ , \tag{4}$$

being I and $\mathbb{I}$ respectively the second and fourth order identity tensors, E the Young's modulus and ν the Poisson's ratio.

In this particular case, we consider that the shape functional $\psi(\Omega)$ in (1) takes the form

$$\psi(\Omega) := \mathcal{J}_\Omega\left(u\right) = \frac{1}{2}\int_\Omega \mathbb{C}\nabla\nabla u\cdot\nabla\nabla u - \int_\Omega bu - \int_{\Gamma_N}\left(\bar{q}u+\bar{m}\frac{\partial u}{\partial n}\right) - \sum_{i=1}^{nv}\bar{Q}_{v_i}u(x_{v_i}) \ , \tag{5}$$

that represents the total potential energy of the plate in the reference configuration Ω and u is the solution to the following variational problem: find $u \in \mathcal{U}$, such that

$$\int_\Omega \mathbb{C}\nabla\nabla u\cdot\nabla\nabla\eta - \int_\Omega b\eta - \int_{\Gamma_N}\left(\bar{q}\eta+\bar{m}\frac{\partial \eta}{\partial n}\right) - \sum_{i=1}^{nv}\bar{Q}_{v_i}\eta(x_{v_i}) = 0 \quad \forall\eta\in\mathcal{V} \ , \tag{6}$$

where the first term represents the virtual strain energy stored in the plate and the other terms the virtual work of the external loads. The set of admissible displacements $\mathcal{U}$ and the space of admissible displacements variations $\mathcal{V}$ are defined as follows

$$\mathcal{U} := \left\{u\in H^2\left(\Omega\right) : u|_{\Gamma_D} = \bar{u} \text{ and } \partial_n u|_{\Gamma_D} = \bar{\theta}\right\} \qquad \text{and} \qquad \mathcal{V} := \left\{\eta\in H^2\left(\Omega\right) : \eta|_{\Gamma_D} = 0 \text{ and } \partial_n \eta|_{\Gamma_D} = 0\right\} \ , \tag{7}$$

where Γ_D and Γ_N respectively are the Dirichlet and Neumann boundaries such that $\Gamma = \Gamma_D \cup \Gamma_N$ is the boundary of Ω, with $\Gamma_D \cap \Gamma_N = \emptyset$; $\bar{u}$ is a displacement and $\bar{\theta}$ a rotation, both prescribed on Γ_D. Moreover, b, $\bar{q}$, $\bar{m}$ and $\bar{Q}_{v_i}$, in Eq. (6) are the system of forces compatible with Kirchhoff's approach, where b is the transverse force over the middle plane Ω, $\bar{q}$ a transverse shear load and $\bar{m}$ is a moment, both prescribed on Γ_N; $\bar{Q}_{v_i}$ is the transverse shear load concentrated at the point $x_{v_i} \in \Gamma_N$ in which there is some discontinuity (vertex, for instance) and nv represents the total number of points x_{v_i}. Finally, $\partial_n(\cdot)$ is used to denote $\nabla(\cdot)\cdot n$, where n is the unit normal vector pointing toward the exterior of Ω.

In our case, we consider a perturbation on the domain characterized by the nucleation of a small circular inclusion of radius ϵ with different Young's modulus with respect to the bulk material. Thus we have a new domain $\Omega_\epsilon = \Omega\backslash B_\epsilon \cup \mathcal{I}_\epsilon$ whose boundary is denoted by $\Gamma_\epsilon = \Gamma \cup \partial\mathcal{I}_\epsilon$, where $\overline{B_\epsilon} = B_\epsilon \cup \partial B_\epsilon$ is a ball of radius ϵ centered at the point $\hat{x} \in \Omega$. Thus, we have the original domain without inclusion Ω and the new one Ω_ϵ with a small inclusion $\mathcal{I}_\epsilon$. Then, we can define a elasticity tensor $\mathbb{C}_\epsilon$ as

$$\mathbb{C}_\epsilon = \gamma_\epsilon\mathbb{C} \ , \tag{8}$$

where γ_ϵ is the contrast defined in this context as:

$$\gamma_\epsilon = \begin{cases} 1 \text{ if } x\in\Omega\backslash\overline{B_\epsilon} \\ \gamma \text{ if } x\in\mathcal{I}_\epsilon \end{cases} \ . \tag{9}$$

Therefore, the shape functional $\psi(\Omega_\epsilon)$ in 1 is given by

$$\psi(\Omega_\epsilon) := \mathcal{J}_{\Omega_\epsilon}(u_\epsilon) = \frac{1}{2}\int_{\Omega_\epsilon} \mathbb{C}_\epsilon \nabla\nabla u_\epsilon \cdot \nabla\nabla u_\epsilon - \int_{\Omega_\epsilon} b u_\epsilon - \int_{\Gamma_N}\left(\bar{q}u_\epsilon + \bar{m}\frac{\partial u_\epsilon}{\partial n}\right) - \sum_{i=1}^{nv} \bar{Q}_{v_i} u_\epsilon(x_{v_i}) \;, \tag{10}$$

that represents the total potential energy of the plate in the perturbed configuration Ω_ϵ and u_ϵ is the solution to the following variational problem: find $u_\epsilon \in \mathcal{U}_\epsilon$, such that

$$\int_{\Omega_\epsilon} \mathbb{C}\nabla\nabla u_\epsilon \cdot \nabla\nabla \eta_\epsilon - \int_{\Omega_\epsilon} b\eta_\epsilon - \int_{\Gamma_N}\left(\bar{q}\eta_\epsilon + \bar{m}\frac{\partial \eta_\epsilon}{\partial n}\right) - \sum_{i=1}^{nv} \bar{Q}_{v_i}\eta_\epsilon(x_{v_i}) = 0 \quad \forall \eta_\epsilon \in \mathcal{V}_\epsilon \;, \tag{11}$$

where the set of admissible displacements $\mathcal{U}_\epsilon$ and the space of admissible displacements variations $\mathcal{V}_\epsilon$ are defined as

$$\mathcal{U}_\epsilon := \{u_\epsilon \in \mathcal{U} : [\![u_\epsilon]\!] = 0, [\![\partial_n u_\epsilon]\!] = 0 \text{ on } \partial\mathcal{I}_\epsilon\} \quad \text{and} \quad \mathcal{V}_\epsilon := \{\eta_\epsilon \in \mathcal{V} : [\![\eta_\epsilon]\!] = 0, [\![\partial_n \eta_\epsilon]\!] = 0 \text{ on } \partial\mathcal{I}_\epsilon\} \,. \tag{12}$$

Lets us introduce the notation $[\![(\cdot)]\!] = (\cdot)|_e - (\cdot)|_i$, that represents the jump of $(\cdot)$ across the boundary of the inclusion $\partial\mathcal{I}_\varepsilon$ and $(\cdot)|_e$ and $(\cdot)|_i$ used to indicate that $(\cdot)$ is being evaluated on the matrix and on the inclusion, respectively. Then, the Euler-Lagrange equation as well as the boundary conditions associated to the variational problem (Eq. 11) are given by the following fourth order boundary-value problem:

Find u_ϵ, such that

$$\left\{\begin{array}{lll}
-\mathrm{div}\,(\mathrm{div} M_\epsilon) = b & \text{in} & \Omega\backslash\overline{B_\epsilon} \\
M_\epsilon = -\mathbb{C}\nabla\nabla u_\epsilon & \text{in} & \Omega\backslash\overline{B_\epsilon} \\
\left.\begin{array}{l} u_\epsilon = \bar{u} \\ \partial_n u_\epsilon = \bar{\theta} \end{array}\right\} & \text{on} & \Gamma_D \\
\left.\begin{array}{l} \partial_t M_\epsilon^{tn} + \mathrm{div} M_\epsilon \cdot n = \bar{q} \\ -M_\epsilon^{nn} = \bar{m} \end{array}\right\} & \text{on} & \Gamma_N \\
M_\epsilon^{tn}|_+ - M_\epsilon^{tn}|_- = \bar{Q}_{v_i} & \text{on} & x_{v_i} \in \Gamma_N, \quad i = 1, ..., nv \quad . \\
-\mathrm{div}\,(\mathrm{div} M_\epsilon) = b & \text{in} & \mathcal{I}_\varepsilon \\
M_\epsilon = \gamma\mathbb{C}\nabla\nabla u_\epsilon & & \\
\left.\begin{array}{l} [\![\partial_t M_\epsilon^{tn}]\!] + [\![\mathrm{div} M_\epsilon]\!]\cdot n = 0 \\ [\![-M_\epsilon^{nn}]\!] = 0 \\ [\![\partial_n u_\epsilon]\!] = 0 \\ [\![u_\epsilon]\!] = 0 \end{array}\right\} & \text{on} & \partial\mathcal{I}_\varepsilon
\end{array}\right. \tag{13}$$

Being $\partial_t(\cdot) = \nabla(\cdot)\cdot t$ and $\partial_n(\cdot) = \nabla(\cdot)\cdot n$. It should be noted that we can decompose the stress tensor M_ϵ along the boundary Γ_ϵ as follows

$$M_\epsilon = M_\epsilon^{nn}(n\otimes n) + M_\epsilon^{nt}(n\otimes t) + M_\epsilon^{tn}(t\otimes n) + M_\epsilon^{tt}(t\otimes t) \;, \tag{14}$$

where n and t are respectively the outward normal and tangential unit vectors ($n\cdot t = 0$) defined on Γ_ϵ.

3. TOPOLOGICAL SENSITIVITY ANALYSIS

In the present section, we compute the topological derivative for the total potential energy shape functional associated to the thin elastic plate bending problem within the framework of Kirchhoff's simplified assumptions.

3.1 Topological Derivative Calculation

Let us state the following result, leading to a constructive method for computing the topological derivatives (Novotny et al. (2003)). The topological derivative given by Eq. (2) can be written as

$$D_T(\hat{x}) = \lim_{\epsilon\longrightarrow 0}\frac{1}{f'(\epsilon)}\frac{d}{d\epsilon}\psi(\Omega_\epsilon) \;, \tag{15}$$

where $\frac{d}{d\epsilon}\psi(\Omega_\epsilon)$ may be seen as the classical sensitivity analysis to the change in shape produced by an uniform expansion of the inclusion. In fact, considering a direct analogy with continuum mechanics we have that the shape derivative of the cost function $\psi(\Omega_\epsilon)$ can be written as

$$\frac{d}{d\epsilon}\psi(\Omega_\epsilon) = \int_{\Gamma_\epsilon} [\![\Sigma_\epsilon]\!] n\cdot v + \int_{\partial\mathcal{I}_\epsilon} [\![M_\epsilon]\!] n\cdot\nabla v^T \nabla u_\epsilon - \int_{\Omega_\epsilon} \mathrm{div}\Sigma_\epsilon \cdot v \;, \tag{16}$$

being v the *shape change velocity* defined as

$$\begin{cases} v = -n & \text{on } \partial\mathcal{I}_\epsilon, \\ v = 0 & \text{on } \Gamma, \end{cases} \tag{17}$$

and Σ_ϵ, can be seen as an extension of the Eshelby's energy-momentum tensor (see for instance Eshelby (1975)) for elastic plates within the framework of Kirchhoff's approach, which is given by

$$\Sigma_\epsilon = -\frac{1}{2}\left(M_\epsilon \cdot \nabla\nabla u_\epsilon + 2bu_\epsilon\right) I + \left(\nabla\nabla u_\epsilon\right) M_\epsilon - \nabla u_\epsilon \otimes \mathrm{div} M_\epsilon \ . \tag{18}$$

Moreover, from Novotny et al. (2005) we have that the tensor Σ_ϵ is divergence free tensor field, that is

$$\int_{\Omega_\epsilon} \mathrm{div}\Sigma_\epsilon \cdot v \ d\Omega_\epsilon = 0 \quad \forall\, v{\in}\Omega_\epsilon \quad \Leftrightarrow \quad \mathrm{div}\Sigma_\epsilon = 0 \ . \tag{19}$$

Then, from (17) the topological derivative becomes

$$D_T\left(\hat{x}\right) = -\lim_{\epsilon\to 0}\frac{1}{f'\left(\epsilon\right)}\left\{\int_{\partial\mathcal{I}_\epsilon}[\![\Sigma_\epsilon]\!]n\cdot n + \int_{\partial\mathcal{I}_\epsilon}[\![M_\epsilon]\!]n\cdot\nabla n^T\nabla u_\epsilon\right\} \ . \tag{20}$$

3.2 Asymptotic analysis

In order to obtain the final expression of the topological derivative, we need to study the behavior of the integral given by Eq. (20) in relation to the parameter ϵ, which may be obtained through an asymptotic analysis of the solution u_ϵ. Then, introducing a polar coordinate system (r,θ) aligned with the principal stress directions and centered at $\hat{x}$, we have the following asymptotic expansion for the stress components

$$M_\epsilon^{nn}\big|_e = S\left(1-\frac{1-\gamma}{1+\gamma\alpha}\frac{\epsilon^2}{r^2}\right) + D\left(1-\frac{1-\gamma}{1+\beta\gamma}\left(\frac{4\nu}{3+\nu}\frac{\epsilon^2}{r^2}+3\beta\frac{\epsilon^4}{r^4}\right)\right)\cos 2\theta + \mathcal{O}(\epsilon) \ , \tag{21}$$

$$M_\epsilon^{tt}\big|_e = S\left(1+\frac{1-\gamma}{1+\gamma\alpha}\frac{\epsilon^2}{r^2}\right) - D\left(1+\frac{1-\gamma}{1+\beta\gamma}\left(\frac{4}{3+\nu}\frac{\epsilon^2}{r^2}-3\beta\frac{\epsilon^4}{r^4}\right)\right)\cos 2\theta + \mathcal{O}(\epsilon) \ , \tag{22}$$

$$M_\epsilon^{nt}\big|_e = -D\left(1-\beta\frac{1-\gamma}{1+\beta\gamma}\left(2\frac{\epsilon^2}{r^2}-3\frac{\epsilon^4}{r^4}\right)\right)\sin 2\theta + \mathcal{O}(\epsilon) \ , \tag{23}$$

$$M_\epsilon^{nn}\big|_i = \frac{2S}{(1-\nu)(1+\gamma\alpha)} + \frac{4D}{(3+\nu)(1+\beta\gamma)}\cos 2\theta + \mathcal{O}(\epsilon) \ , \tag{24}$$

$$M_\epsilon^{tt}\big|_i = \frac{2S}{(1-\nu)(1+\gamma\alpha)} - \frac{4D}{(3+\nu)(1+\beta\gamma)}\cos 2\theta + \mathcal{O}(\epsilon) \ , \tag{25}$$

$$M_\epsilon^{nt}\big|_i = -\frac{4D}{(3+\nu)(1+\beta\gamma)}\sin 2\theta + \mathcal{O}(\epsilon) \ , \tag{26}$$

where

$$S = \frac{m_1+m_2}{2}, \quad D = \frac{m_1-m_2}{2}, \quad \alpha = \frac{1+\nu}{1-\nu} \quad \text{and} \quad \beta = \frac{1-\nu}{3+\nu} \ , \tag{27}$$

m_1 and m_2 are eigenvalues (the principal bending moments) of the generalized stress (bending moment) tensor M (associated to the original domain without inclusion Ω) evaluated at the point $\hat{x}\in\Omega$, that is $M|_{\hat{x}}$.

Next, by substituting the above expansions into Eq. (20), we observe that $f'\left(\epsilon\right) = \mathrm{meas}\left(\partial B_\epsilon\right) \ \Rightarrow \ f\left(\epsilon\right) = \mathrm{meas}\left(B_\epsilon\right)$ and we can finally compute the limit $\epsilon\to 0$ in Eq. (20) which becomes

$$D_T\left(\hat{x}\right) = \frac{6(1-\gamma)}{E\rho^3}\left[\frac{\left(m_1+m_2\right)^2}{1+\gamma\alpha} + 2\frac{\alpha\beta}{1+\gamma\beta}\left(m_1-m_2\right)^2\right] \ . \tag{28}$$

On the other hand m_1 and m_2 are given by

$$m_{1,2} = \frac{1}{2}\left(\mathrm{tr}M \pm \sqrt{2M^D\cdot M^D}\right) \ , \tag{29}$$

where M^D is the deviatory part of the stress-tensor M, that is

$$M^D = M - \frac{1}{2}\mathrm{tr}\left(M\right) I \ . \tag{30}$$

Further substituting Eqs. (29, 30) into Eq. (28), we have that

$$D_T(\hat{x}) = \frac{6(1-\gamma)}{E\rho^3}\left(4\frac{\alpha\beta}{1+\gamma\alpha}M\cdot M + \left(\frac{1}{1+\gamma\alpha} - 2\frac{\alpha\beta}{1+\gamma\beta}\right)(\mathrm{tr}M)^2\right) . \tag{31}$$

Finally, we can rewrite the topological derivative as a function of the tensors M and $\nabla\nabla u$ by means of the constitutive equation and a simple manipulation, which leads to

$$D_T(\hat{x}) = -\mu\alpha\frac{1-\gamma}{1+\gamma\beta}\left(4\beta M\cdot\nabla\nabla u + \left(\frac{1-2\beta+\gamma\beta(1-2\alpha)}{1+\gamma\alpha}\right)\mathrm{tr}M\,\mathrm{tr}\nabla\nabla u\right) , \tag{32}$$

where $\mu = \frac{1}{2(1+\nu)}$. It should be noted that M and $\nabla\nabla u$ are associated to the unperturbed domain Ω and that we have assumed $b = 0$.

3.3 Numerical Verification

In order to verify the topological derivative formulae we have considered a unit square plate, simply supported at the corners, with thickness $\rho = 0.05$ and Young's module $E = 1.0$. With this data we used the Eq. (2) to perform a sequence of finite element analyses to obtain $\psi(\Omega_\epsilon)$ considering inclusions of radii

$$\epsilon \in \{0.08, 0.04, 0.02, 0.01\}, \tag{33}$$

centered at $\hat{x} = (0.5, 0.5)$. The solutions u and u_ϵ are calculated via the Finite Element Method. More specifically, in the numerical experiments we have adopted the DKT finite element (*Discrete Kirchhoff Triangle*, Batoz (1982)). The finite element mesh used contains 12730 nodes and 25322 elements. Figure 1 shows the mesh and the domain with a bilinear bending distribution along the edges of the plate where the numbers represent the maximum values of the bending moments at a distance $a = 0.10$ from the corners.

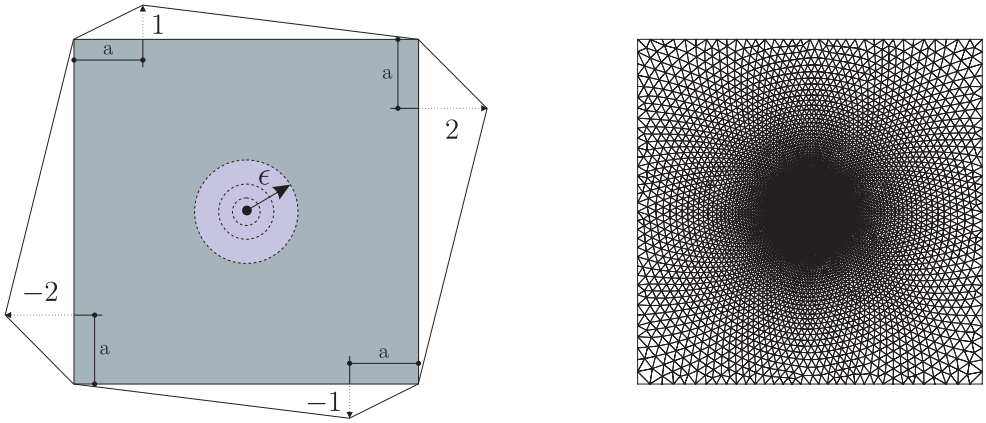

(a) Domain (b) Finite element mesh.

Figure 1. Numerical Verification

We have calculated the topological derivative for the cases: $\gamma = \{0.1, 0.5, 2, 10\}$. The results are shown in the Fig. 2 where the analytical value of the topological derivative (28) was calculated and compared with the asymptotic behavior of the eq. (2) for the decreasing values of ϵ.

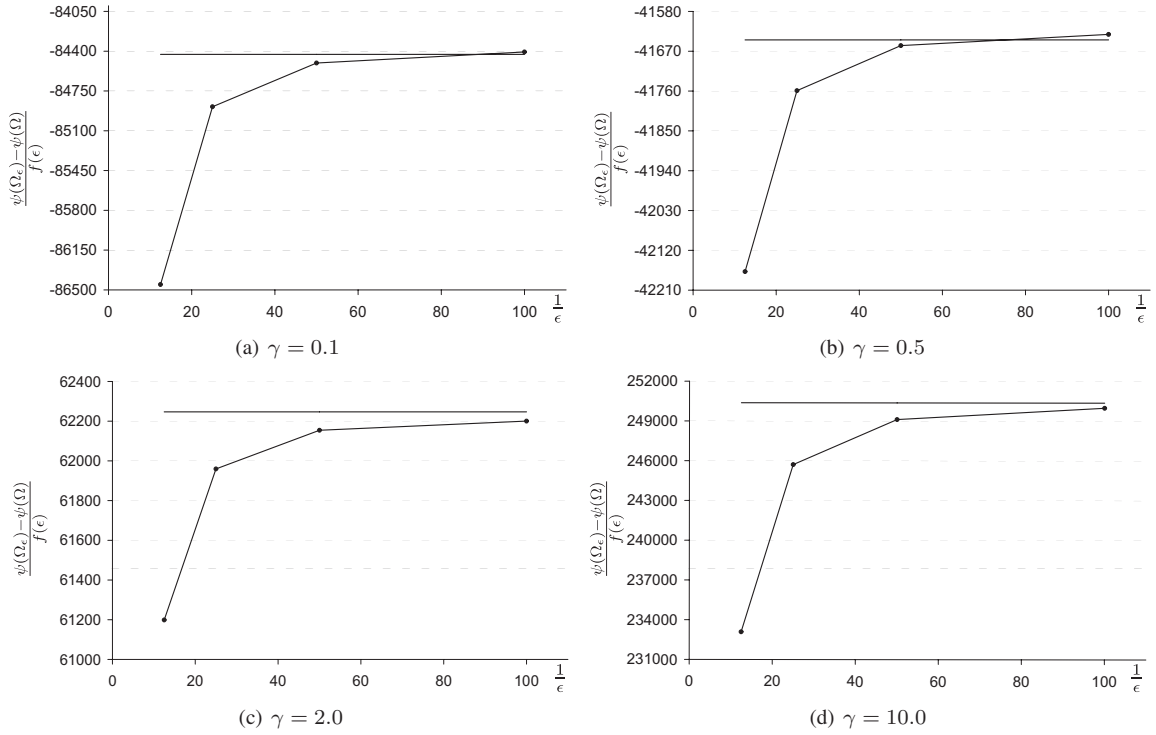

(a) $\gamma = 0.1$ (b) $\gamma = 0.5$

(c) $\gamma = 2.0$ (d) $\gamma = 10.0$

Figure 2. Topological derivative verification.

4. NUMERICAL EXPERIMENTS

In Section 3 we have calculated the topological derivative for the total potential strain energy associated to the Kirchhoff's plate bending problem with respect to the nucleation of a circular inclusion. The topological derivative, in this context, indicates the best place to insert or remove material in order to minimize the total potential energy. Therefore, this information can be used as an alternative method to perform the topology design of plate components. In particular, the main idea is to change materials (more rigid $\leftrightarrow$ less rigid) where $|D_T(\hat{x})|$ assumes smallest/higher values. For classical methods of topology optimization based on relaxed formulations we refer the reader to the fundamental paper by Bendsøe and Kikuchi (1988) and its further development.

In order to proceed, the field $D_T(\hat{x})$ is evaluated at the nodal points of the finite element mesh, being that we interchange the material properties in the elements that share the node which satisfies $\xi_{\text{inf}} \leq D_T(\hat{x}_K) \leq \xi_{\text{sup}}$, where $\hat{x}_K$ is the K-th nodal point of the finite element mesh.

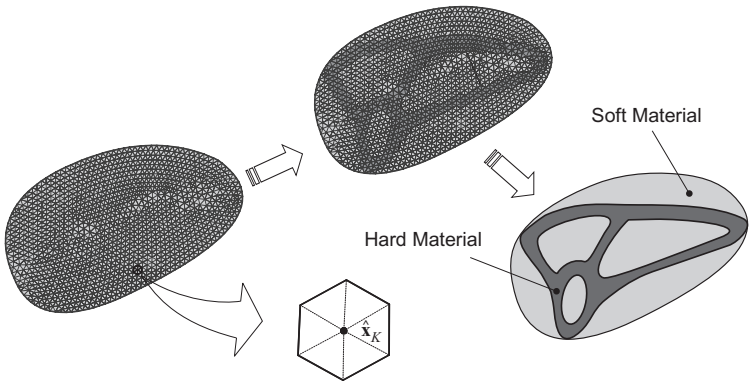

Figure 3. Sketch of the adopted procedure of inserting and to removing material in a finite element mesh.

In this example, we have a square plate supported by a column at its center submitted to concentrated loads $\bar{Q} = 100$ at the corners (Fig. 4 with $R = 50$). Considering the symmetry of the problem, the initial domain $\overline{\Omega} = [0, 250] \times [0, 250]$ is discretized in 35094 finite elements and 17794 nodes. The algorithm used allows us to insert and remove material in an iterative process and was proposed by Giusti et al. (2008). In particular, we interchange 1% of hard to soft materials at each step until the volume constraint is reached, then we reduce the step size to 0.25% and continue the iterative process. The Young's modulus $E = 210 \times 10^3$, Poisson's ratio $\nu = 0.3$, thickness $\rho = 5$ and the contrast $\gamma = 10^{-2}$ are assumed.

Furthermore, the region that appears in white is not perturbed and the thick line and the line-dot that appear on the figures are respectively used to denote clamped ($u = \partial_n u = \partial_t u = 0$) and symmetry ($\partial_n u = 0$) boundary conditions.

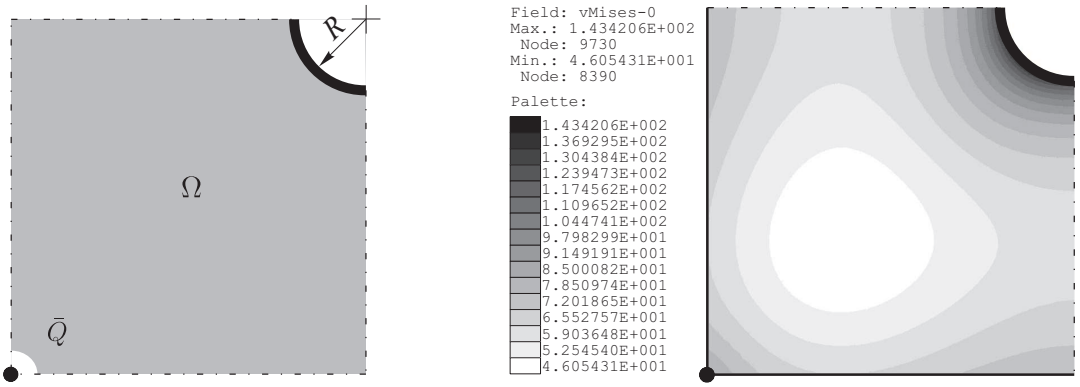

(a) model (b) von Mises stress field

Figure 4. Model and stress distribution

Considering the volume constraint given by 50% of the initial volume, in Fig. 5 we show the obtained results. The relative value of the shape functional at each iteration j, $\psi\left(\Omega^j\right)$, throughout the optimization procedure is presented in Fig.6. The history of the hard material volume during the iterative process can be observed in Fig. 7. The comparison between the values of the von Mises stress field obtained at iterations $j = \{38, 395\}$ can be observed in Fig. 8.

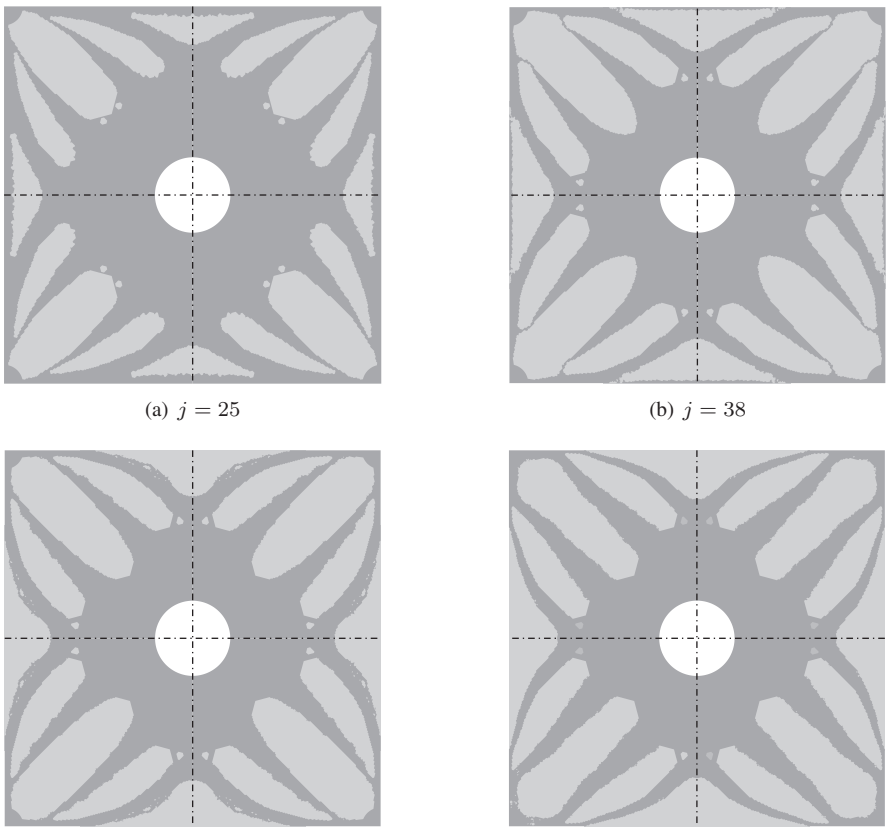

(a) $j = 25$ (b) $j = 38$

(c) $j = 239$ (d) $j = 395$

Figure 5. Obtained topologies during the iterative process

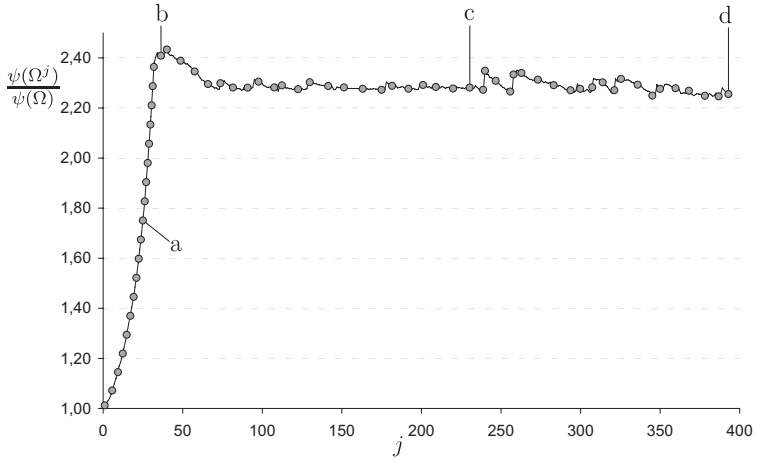

Figure 6. Relative values of the shape functional during the iterative process.

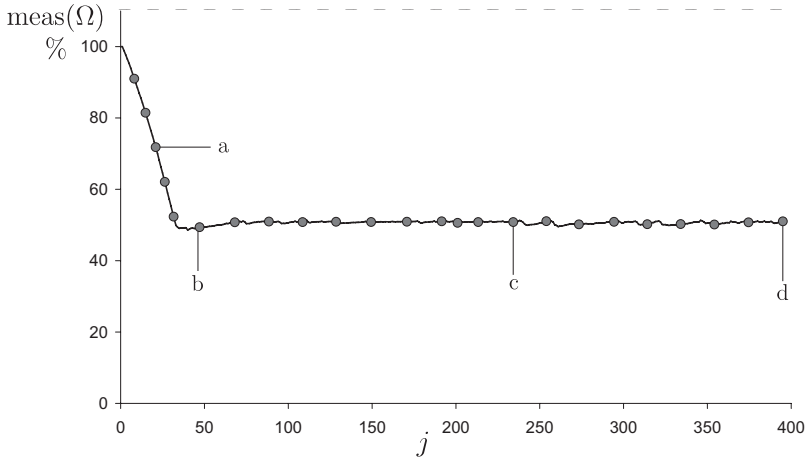

Figure 7. Volume fraction of the hard material during the iterative process.

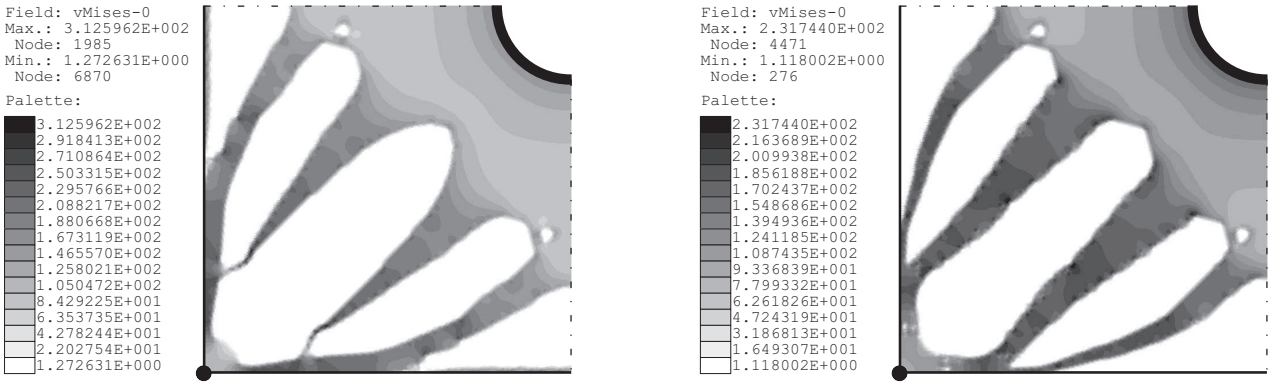

(a) $j = 38$ (b) $j = 395$

Figure 8. von Mises stress fields.

As a conclusion of this numerical experiment we observe that once the volume constraint is reached, the algorithm insert and remove material simultaneously, preserving the current volume fraction, in order to minimize the total potential energy. As a consequence we obtain a configuration in which the bending moments are more uniformly distributed. In other words, the stress field is redistributed, as can be seen in Fig. 8, leading to a reduction of more than 25% in its maximum value. This procedure leads to better results than the ones obtained in Novotny et al. (2005) simply by removing material.

5. Conclusions

An analytical expression for the topological derivative associated to the total potential energy for the Kirchhoff's plate bending problem, when a circular inclusion of a material with different Young's modulus is introduced at an arbitrary point of the domain, has been proposed in this paper. In order to verify the obtained analytical expression, we have developed a numerical validation showing the convergence of the numerical topological derivative to their corresponding analytical value. The obtained result was used as a steepest descent direction in a topology design algorithm. Finally, we have presented a numerical experiment showing the potentialities of the proposed methodology in the context of Kirchhoff's plate structural design.

6. ACKNOWLEDGEMENTS

This research was financially supported by Brazil/France program CAPES/COFECUB under the grant 604/08. S.M. Giusti was supported by CNPq under grant 382485/2009-2, and D.E. Campeão was supported by PIBIC/LNCC-CNPq. This support is gratefully acknowledged.

7. REFERENCES

Allaire, G., Gournay, F., Jouve, F., Toader, A., 2005. Structural optimization using topological and shape sensitivity via a level set method. Control and Cybernetics 34 (1), 59–80.

Amstutz, S., Andrä, H., 2006. A new algorithm for topology optimization using a level-set method. Journal of Computational Physics 216 (2), 573–588.

Amstutz, S., Horchani, I., Masmoudi, M., 2005. Crack detection by the topological gradient method. Control and Cybernetics 34 (1), 81–101.

Auroux, D., Masmoudi, M., Belaid, L., 2007. Image restoration and classification by topological asymptotic expansion. In: Variational formulations in mechanics: theory and applications. Barcelona, Spain.

Batoz, J. L., 1982. An explicit formulation for an efficient triangular plate-bending element. Advances in Applied Mechanics 18, 1077–1089.

Bendsøe, M., Kikuchi, N., 1988. Generating optimal topologies in structural design using an homogenization method. Computer Methods in Applied Mechanics and Engineering 71 (2), 197–224.

Eshelby, J., 1975. The elastic energy-momentum tensor. Journal of Elasticity 5 (3-4), 321–335.

Feijóo, G., 2004. A new method in inverse scattering based on the topological derivative. Inverse Problems 20 (6), 1819–1840.

Giusti, S., Novotny, A., Padra, C., 2008. Topological sensitivity analysis of inclusion in two-dimensional linear elasticity. Engineering Analysis with Boundary Elements 32 (11), 926–935.

Larrabide, I., Feijóo, R., Novotny, A., Taroco, E., 2008. Topological derivative: a tool for image processing. Computers & Structures 86 (13-14), 1386–1403.

Lee, S., Kwak, B., 2008. Smooth boundary topology optimization for eigenvalue performance and its application to the design of a flexural stage. Enginnering Optmization 40 (3), 271–285.

Nazarov, S., Sokołowski, J., 2003. Asymptotic analysis of shape functionals. Journal de Mathématiques Pures et Appliquées 82 (2), 125–196.

Novotny, A., Feijóo, R., Padra, C., Taroco, E., 2003. Topological sensitivity analysis. Computer Methods in Applied Mechanics and Engineering 192 (7-8), 803–829.

Novotny, A., Feijóo, R., Padra, C., Taroco, E., 2005. Topological derivative for linear elastic plate bending problems. Control and Cybernetics 34 (1), 339–361.

Sokołowski, J., Żochowski, A., 1999. On the topological derivatives in shape optmization. SIAM Journal on Control and Optimization 37 (4), 1251–1272.

8. Responsibility notice

The authors are the only responsible for the printed material included in this paper.